

# THE RHIC INJECTION KICKER

CONF970503--90

H. Hahn\*, N. Tsoupas, and J. E. Tuozzolo, Brookhaven National Laboratory, Upton, New York 11973

## Abstract

Beam transfer from the AGS to RHIC is performed in single-bunch mode. Close spacing of the bunches in the collider requires an injection kicker with a rise time of  $<90$  nsec, suggesting adoption of a travelling wave structure. The required vertical kick of  $0.186$  T-m is provided by 4 magnets, each  $1.12$  m long with a  $48.4 \times 48.4$  mm aperture and operated at  $1.6$  kA. The kicker is constructed as a "C" cross section magnet, in which ferrite and high-permittivity dielectric sections alternate. The dielectric blocks provide the capacity necessary for the nominally  $25 \Omega$  characteristic impedance of the travelling wave structure, but impose the practical limit on the peak voltage, and thus current, achievable. Computer studies to minimize local electric field enhancements resulted in a configuration capable of holding  $\sim 50$  kV, with adequate safety margin over the nominal  $40$  kV. Equivalent circuit analysis indicated the possibility of lowering the nominal voltage by operating mismatched into  $20 \Omega$  terminations without degrading the pulse shape. In this paper, the experience gained in the fabrication of the production units and the results from various single-unit tests and operation of four kickers with beam in the "Sextant Test" are reported.

## 1 INTRODUCTION

The design of the RHIC injection system was dominated by the requirements of the strength and risetime of the fast kicker. The kicker has to provide a vertical deflection of  $1.86$  mrad for beams with a  $B\rho = 100$  Tm. The available free space for the four kickers limits their effective length to  $1.12$  m each. Neglecting any contribution from the electric field, the deflecting magnet field is required to be  $415$  G inside the beam tube. This leads, with the horizontal aperture of  $4.84$  cm, to the current requirement of  $1.6$  kA. The kickers are each powered from a Blumlein pulser which is designed for  $50/2 \Omega$ , imposing a characteristic impedance of  $25 \Omega$  and a nominal voltage of  $\sim 40$  kV in the kicker. Injecting beam from the AGS to RHIC is performed by single-bunch transfer into stationary buckets of the acceleration rf system at  $24.15$  MHz. Transfer of  $120$  bunches, as intended in a design upgrade, requires filling of every third bucket, spaced  $107$  nsec apart. The ion bunches are expected to be  $<15$  nsec long, leading to a risetime requirement ( $1 - 9\%$ ) of  $<90$  nsec in deflection or  $\sim 45$  nsec in current. During the bunch length, the flat top requirement is  $\pm 1\%$ , easily achieved with the  $100$  nsec long pulse. At the end of the injection process, a gap of  $\sim 1 \mu\text{sec}$  will be left to facilitate

the beam abort, implying that there is no severe constraint on the fall time.

The risetime requirement suggested the adoption of a transmission line structure. Using a CERN-type "plate-kicker" is the quasi-standard solution to achieve fast rise times.<sup>1</sup> Replacing its lumped capacitors by high-permittivity ceramic blocks promised to be simpler, more compact, and thus more economical. Following concepts contemplated at SLAC,<sup>2,3</sup> the original design for the RHIC injection kicker was generated by Forsyth, et al.<sup>4</sup> The kicker R&D program with the results from half-length models demonstrated the viability of this solution. However, it became evident that the specifications for the RHIC kicker are at the limit of what can be expected from this type of kicker; furthermore sharp resonances in the coupling impedance made appropriate design changes imperative.<sup>5</sup> A modified design of the kicker core and the development of special tooling and fabrication procedures then made the production of full-size kickers for operation in the "Sextant Test" possible.

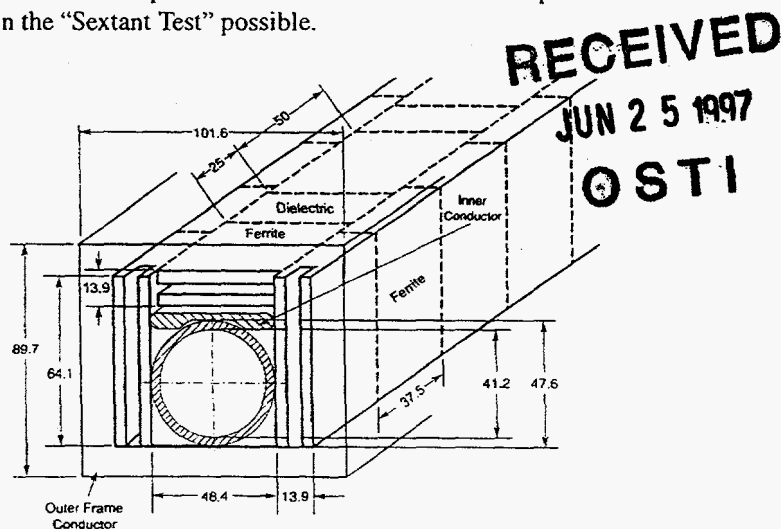


Figure 1: RHIC injection kicker configuration (Dimensions in mm). Only the end blocks are slotted.

## 2 KICKER CONFIGURATION

The kicker is configured as a "C" magnet with interspersed ferrite<sup>6</sup> and dielectric<sup>7</sup> blocks as shown in Fig. 1. On the top, there are  $14 \times 1$  in. dielectric and  $15 \times 2$  in. ferrite blocks. The field in the ferrite reaches here  $2.13$  kG at the nominal  $415$  G in the gap. The ferrite in the sides, although in principle continuous, must be assembled from  $1.5$  in. long blocks to avoid eddy currents.

\* Work performed under the auspices of the U.S. Department of Energy

MASTER

DISTRIBUTION OF THIS DOCUMENT IS UNLIMITED

The design objective of 40 kV across the 1.39 cm thick blocks results in a nominal field of 29 kV/cm. This is below published values,  $\sim 60$  kV/cm, for similar dielectrics such as sintered titania-rutil,<sup>8</sup> or barium titanate.<sup>9</sup> However, the manufacturers of our materials provided no information (or warranty) as to their electric breakdown limits. Thus, prior to their assembly, all incoming blocks were tested in Fluorinert between parallel plates to 60 kV with millisecc pulses. The test voltage for the dielectric and ferrite blocks is thus 50% above the nominal design requirement. There is reason to assume, that higher fields can be reached with nanosecc pulses, especially in the ferrite where eddy currents play an important role.

The nominal electrical field of 29 kV/cm is also significantly below the reported electric breakdown strengths of epoxy and RTV ( $\sim 300$  kV/cm).<sup>10</sup> Epoxy is used to form the magnet core consisting of the ferrite/dielectric blocks with the busbar (i.e. the inner conductor), and RTV is used in the final assembly of the core into the frame. However, due to the large ratio of  $\epsilon_{\text{diel}}/\epsilon_{\text{epoxy}} \sim 30$ , correspondingly larger fields can exist in an epoxy layer over the dielectric and must be avoided. Prior to its final assembly the kicker core is machine-ground with a diamond wheel to remove any epoxy from the surface and to assure direct contact via an indium layer with the frame.

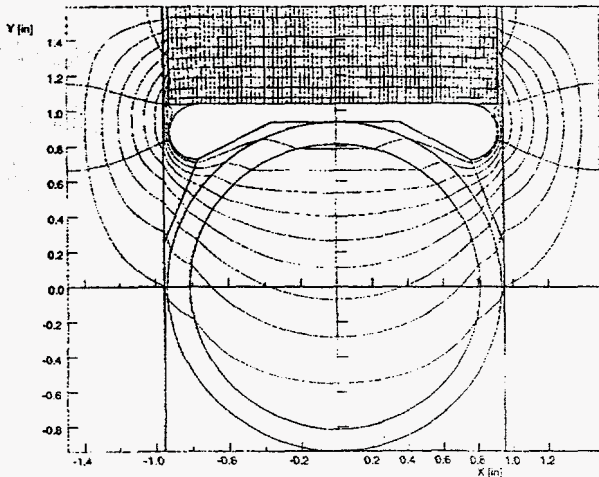


Figure 2: Electric field lines in a cross section at the center of the dielectric blocks.

Searching for a solution which minimizes local field enhancements while retaining a maximum capacitance lead to an extensive experimental and theoretical R&D program. Electrostatic computations using the OPERA-2d program were performed to establish the peak electric fields and their location in the core. The design was optimized by focussing on the geometry of the dielectric block and the details of its contact with the busbar, established by a 4 mil indium layer. The obvious ideal condition is a dielectric block between two infinite parallel plates, but finding the best approximation required numerous computa-

tions and their experimental verification by tests on almost a dozen half-length models. Tests were done on magnet cores with dielectric blocks ranging from 1.5 to the original 3 in. width while maintaining the same overall dimensions and busbar geometry. The two-dimensional electric field lines and equipotentials in a cut through the center of the dielectric block is shown in Fig. 2.

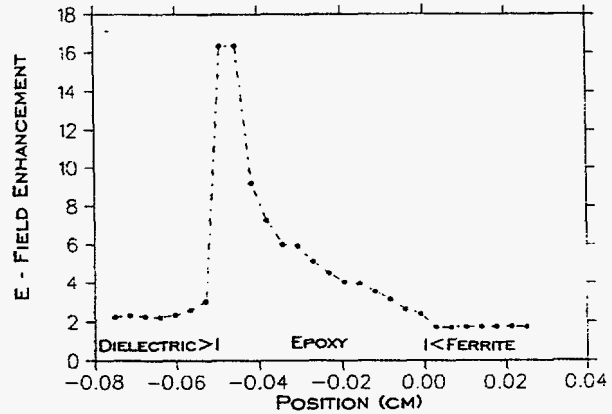


Figure 3: Electric field components on a line in beam direction through the dielectric block (at left), the epoxy layer, and the ferrite block (at right).

The boundary conditions of the time-varying electric components of the TEM mode in the kickers are identical to those of two-dimensional static electric fields. Thus the electrostatic field computations with the OPERA-2 program provide correct results for the pulsed electric fields at the center of the blocks, and a good approximation over a large fraction of the blocks. However, the fields at the ferrite-dielectric interface are three-dimensional and have been addressed by separate computations. The electric field components on a line in beam direction through the blocks at the location of the peak field is shown in Fig. 3. The results confirmed the assumption that the disturbance due to the epoxy layer is highly localized and that the fields are essentially two-dimensional in the blocks. The three-dimensional peak field enhancement in the dielectric blocks of the present design were found to be 3.5 at the corner versus the 2.2 at the center.

### 3 KICKER PERFORMANCE

As of today, six full-size production kickers have been built. The first four were assembled with MCT-100 blocks resulting in a characteristic impedance of  $28.6 \Omega$ . Starting with kicker #5, MCT-125 blocks were used in order to reduce the impedance to  $\sim 25 \Omega$ .

Direct measurement of the kicker performance without beam is effectively limited to the current in the termination load and the Blumlein charging voltage, but its value is not rigorously equal to the voltage at the kicker input end. Half-length models were tested at 50 kV for  $\sim 1$  M pulses without degradation, and all production units are verified

to reach the nominal 40 kV. In the Sextant Test, the kicker magnets were terminated with 20 instead of the nominal 25  $\Omega$  as a precaution in order to gain safety margin against voltage breakdown. An equivalent circuit analysis substantiated the observation that the current pulse shape is only minimally changed.<sup>11</sup> The measured load current in kicker #5, terminated with 20  $\Omega$  is shown in Fig. 4 and with a different time scale in Fig. 5. The mismatch causes an "after-pulse," about 850 nsec after the peak of the deflection, due to a reflected signal returning to the pulser and there being reflected again. The after-pulse, by serendipity, falls between the 4th and 5th beam pulse after the injected bunch, if the design 60-bunch injection is attempted. In any case, the after-pulse falls within the  $\sim 1 \mu\text{sec}$  beam dump gap. Measurements in the Sextant Test with beam confirmed that 1.6 kA (or  $\sim 32 \text{ kV}$  across the 20  $\Omega$ ) provide the required deflecting strength with a risetime of  $< 90 \text{ nsec}$ .<sup>12</sup>

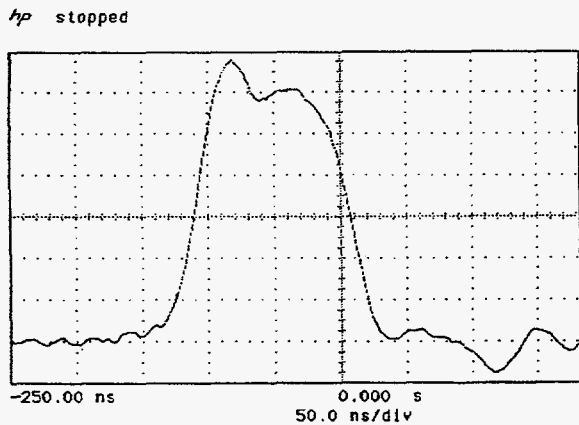


Figure 4: Load current.

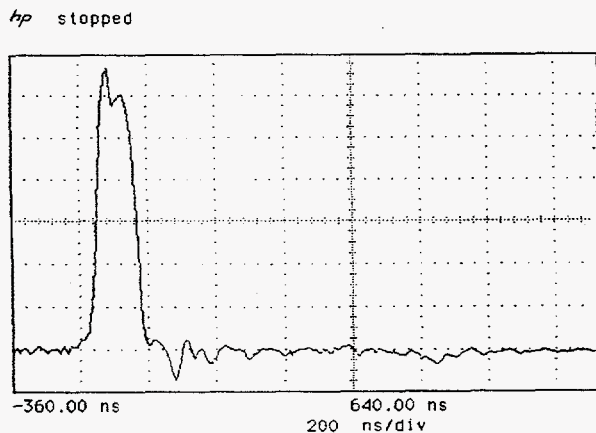


Figure 5: Load current with "after pulse" at 850 nsec.

#### 4 ACKNOWLEDGEMENTS

The authors would like to thank A. Bera, K. Hartmann, C. Rhein, J. Slavik, J. Walsh, A. Wisowaty, and R. Zapasek for their efforts during the R&D program and the manufacturing and testing of the production magnets.

#### 5 REFERENCES

- [1] D. Fiander, Proc. 1971 IEEE Part. Acc. Conf., Chicago, Ill., p. 1022.
- [2] F. Bulos and A. Odian, Report SLAC-PUB-3453, CN-279 (1984).
- [3] R. Cassel (private communication).
- [4] E. B. Forsyth, et al, Proc. 1995 Part. Acc. Conf., Dallas, TX, p. 1921.
- [5] H. Hahn, N. Tsoupas, J. E. Tuozzolo, BNL Report AD/RHIC/RD-109 (1997).
- [6] CMD-5005, Nickel-Zinc ferrite with high permeability and resistivity for use at frequencies up to  $\sim 100 \text{ MHz}$  and a dielectric constant of  $\epsilon \sim 10$ , Ceramic Magnetics, Fairfield, NJ.
- [7] MCT-125, Sintered mixture of Magnesium Titanate and Calcium Titanate with high dielectric constant  $\epsilon \sim 125$ , Trans-Tech, Adamstown, MD.
- [8] Gmelins Handbuch - Titan, vol. 41, p. 250, (Verlag Chemie, Germany, 1951).
- [9] B. Ritscher, Valvo Berichte, vol. VIII-4, p. 110 (1962).
- [10] F. B. A. Fruengel, "High Speed Pulse Technology," (Academic Press, 1980) vol. 1, p 12.
- [11] H. Hahn and A. Ratti, "Equivalent Circuit Analysis" (these proceedings) and BNL Report AD/RHIC/RD-112 (1997).
- [12] W. Fischer, et al (these proceedings).

---

## **DISCLAIMER**

This report was prepared as an account of work sponsored by an agency of the United States Government. Neither the United States Government nor any agency thereof, nor any of their employees, makes any warranty, express or implied, or assumes any legal liability or responsibility for the accuracy, completeness, or usefulness of any information, apparatus, product, or process disclosed, or represents that its use would not infringe privately owned rights. Reference herein to any specific commercial product, process, or service by trade name, trademark, manufacturer, or otherwise does not necessarily constitute or imply its endorsement, recommendation, or favoring by the United States Government or any agency thereof. The views and opinions of authors expressed herein do not necessarily state or reflect those of the United States Government or any agency thereof.

**DISCLAIMER**

**Portions of this document may be illegible  
in electronic image products. Images are  
produced from the best available original  
document.**